

SYNTHESIS AND CHARACTERIZATION OF ACRYLIC BONE CEMENT REINFORCED WITH ZIRCONIA-BIOCERAMIC

D. E. BACIU*, J. SIMITZIS, D. GIANNAKOPOULOS

National Technical University of Athens, School of Chemical Engineering, Department III "Materials Science and Engineering", Laboratory Unit "Advanced and Composite Materials", 9 Heroon Polytechniou str., Zografou Campus, 157 73 Athens, Greece

Acrylic bone cement reinforced with bioceramic was synthesized by mixing beads of PMMA (produced by suspension polymerization), methylmethacrylate (MMA) as monomer, benzoyl peroxide (BPO) as free radical initiator and tetragonal stabilized ZrO₂ powder as bioceramic. The latter was produced by the sol-gel method starting from a proper solution and stabilized in tetragonal phase by digestion treatment with 5M NaOH following heat treatment at 700 °C (tetragonal stabilized zirconia). The structure of PMMA, the structure of tetragonal stabilized zirconia and that of the acrylic bone cement reinforced or not with bioceramic was characterized by Fourier transform infrared spectroscopy (FTIR), X-ray diffraction (XRD) and scanning electron microscopy (SEM).

(Received September 24, 2012; Accepted November 7, 2012)

Keywords: Bioceramics, bone cements, FTIR, XRD, SEM

1. Introduction

Acrylic bone-cements of poly(methylmethacrylate) (PMMA) have been used for more than 40 years in dental implantology for expansion of dental implants, at maxillofacial prosthesis as gentamicin loaded beads, at prosthetics for fixing partial dentures and in orthopaedic surgery for the fixation of artificial joints with encouraging results [1, 2]. In orthopaedic surgery, bone cements serve as a mechanical interlock between the metallic prosthesis and the bone, acting as a load distributor between the artificial implant and the bone [3, 4]. However, local tissue damage due to chemical reactions during polymerization, the high shrinkage of the cement after polymerization, the stiffness mismatch between the bone and the cement, limited mechanical properties and poor compatibility with bone are some drawbacks associated with PMMA-based bone cements [5, 6]. Therefore, improvements in the cement properties are necessary to increase the longevity (performance) of a cemented prosthesis [2]. In this sense, a wide variety of approaches have been used to improve the properties of PMMA bone cements, including the addition of a reinforcing particle or fiber such as carbon fibers, hydroxyapatite particles or fibers, PMMA fibers, stainless steel fibers and titanium fibers, among others [7]. Furthermore, bioactive bone cements including calcium phosphate cements and polymeric cements with bioactive fillers have been reported as alternatives to the common acrylic bone cements. The choice to include a bioactive additive in combination with the acrylic polymer is attractive due to its bone bonding ability and its contribution to more appropriate properties of the composite [8].

Bioceramics such as zirconia, alumina, porcelains, glass-ceramics have been widely used in medical applications due to their superior biocompatibility, aesthetics, mechanical resistance, corrosive resistance and their ease fabrication of complex shapes [9].

Zirconia is considered an excellent ceramic for biomedical application due to its biocompatibility, bioactivity, chemical and dimensional stability, high flexural strength and

* Corresponding author: dianabaciuro@yahoo.com

fracture toughness. Zirconia exists in three crystalline phases: monoclinic, tetragonal and cubic. Regarding the bioactivity of zirconia-based material, it was reported that zirconia gel with tetragonal or monoclinic structure exhibited higher apatite-forming ability in SBF fluids than amorphous gel [10, 11].

In this work, an acrylic bone cement reinforced with bioceramic was prepared by mixing beads of PMMA (produced by suspension polymerization), methylmethacrylate (MMA) monomer, benzoyl peroxide (BPO) as free radical initiator and stabilized ZrO_2 powder acting as bioceramic. The latter was produced by the sol-gel method and stabilized in tetragonal phase.

2. Experimental

2.1. Preparation of the tetragonal stabilized zirconia

The stabilized ZrO_2 powder as bioceramic was produced by the sol-gel method starting from a proper solution and stabilized in tetragonal phase by digestion treatment with 5M NaOH (Sigma Aldrich) following heat treatment at 700 °C (tetragonal stabilized zirconia). The procedure was similar to that of Aguila et al. [12]. Briefly, 50 ml of a 70% propanol solution of zirconium isopropoxide (Sigma-Aldrich) were added slowly drop wise to a mixture of 135 ml of n-propanol (Fluka) and 8 ml of distilled H_2O in a 500 ml round-bottom flask and the suspension was refluxed at 70 °C for 12h. The solid formed was dried in an electrical air oven at 105 °C overnight. The hydrous zirconia obtained was ground, sieved and used for the next procedure concerning the digestion treatment in basic medium.

For the digestion treatment in basic medium, 6 g samples of the hydrous zirconia were placed in round-bottom flasks and refluxed at 100 °C for 9 h in the presence of a 60 ml of a 5 M solution of NaOH. The solids obtained were filtered, washed and dried in an oven at 105 °C.

After drying, part of the samples treated with NaOH were heat treated at 150 °C for 2h and then at 700 °C for 3 h in an electric furnace under air atmosphere in order to obtain stabilized tetragonal stabilized zirconia.

The structure of the tetragonal stabilized zirconia was investigated by FTIR, XRD and SEM.

2.2. Preparation of PMMA beads

PMMA beads were prepared by free radical suspension polymerization [13, 14]. The raw materials: water, suspending agent (CMC) (Fluka), monomer (MMA)(Fluka) and initiator (BPO)(Merck) were added in a 1L three-necked reactor equipped with a reflux condenser, a mechanical stirrer and a temperature control system. The polymer was received as beads and after sieving its portion less than 16 μm was used.

The produced PMMA was characterized by FTIR, XRD and scanning electron microscopy (SEM).

2.3. Preparation of the acrylic bone cement reinforced or not with bioceramic (ZrO_2 powder).

The acrylic bone cement reinforced with bioceramic was prepared by mixing beads of PMMA (produced by suspension polymerization), methylmethacrylate (MMA) as monomer, benzoyl peroxide as free radical initiator and stabilized ZrO_2 powder as bioceramic. Bioceramic powder (ZrO_2 powder in 22.5 % w/w) was added to a solution of PMMA beads (2 g) in MMA (4 ml) with benzoyl peroxide as free radical initiator (0.5 % w/v of MMA). The components of the acrylic bone cement reinforced or not with bioceramic were hand-mixed for ca. 5 min until the mixture became a paste with high viscosity. Then, the paste was placed into small parallelepiped moulds and polymerized at 60 °C for 24 hours to give acrylic bone cement or acrylic bone cement reinforced with bioceramic.

The structure of the acrylic bone cement reinforced or not with bioceramic (ZrO_2 powder) was investigated by FTIR, XRD and SEM.

Characterization of the materials by FTIR, XRD, SEM/EDS.

FTIR spectra were recorded using a Perkin Elmer Spectrum 2000, on discs prepared by mixing of the sample powder and KBr.

XRD measurements were performed with a Siemens D5000 X-Ray Diffractometer by using sample of the material as powder.

The SEM studies were carried out in a FEI Quanta 200 Scanning Electron Microscope (SEM). The material was examined as specimen with dimensions of 10x8x4mm.

3. Results and discussion

3.1. Tetragonal stabilized zirconia- results

FTIR

Fig. 1 shows the FTIR spectrum of the tetragonal stabilized zirconia (treated with 5M NaOH) after heat treatment at 700 °C.

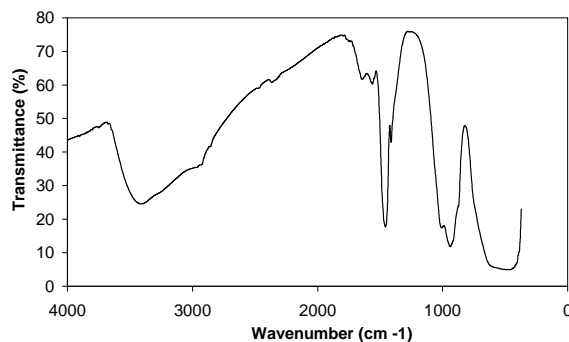


Fig. 1. FTIR spectrum of the tetragonal stabilized zirconia (treated with 5M NaOH) after heat treatment at 700 °C.

According to Fig. 1, the peak at 501 cm^{-1} is assigned to Zr-O stretching modes [15, 16, 17]. The peak at 994-931 cm^{-1} is attributed to the Na-O stretching band [18]. The peaks at 1452 cm^{-1} and 2846-2944 cm^{-1} are attributed to the stretching bands of the hydrocarbon chain [19]. The peaks at 1633 -1555 cm^{-1} and 3403 cm^{-1} are attributed to the bending and stretching vibration of H_2O , respectively [15, 19, 20].

XRD

Fig. 2 shows the XRD results of the tetragonal stabilized zirconia (treated with 5M NaOH) after heat treatment at 700 °C.

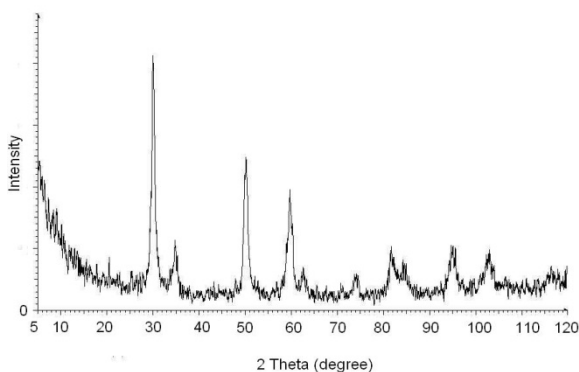


Fig. 2. XRD diffractogram of the tetragonal stabilized zirconia (treated with 5M NaOH) after heat treatment at 700 °C.

According to the diffraction peaks shown in *Fig. 2*, the corresponding d spacings (\AA) were determined: 2.93 ($2\theta=30.3^\circ$), 2.57 ($2\theta=34.8^\circ$), 2.09 ($2\theta=43.1^\circ$), 1.80 ($2\theta=50.4^\circ$), 1.79 ($2\theta=50.9^\circ$), 1.55 ($2\theta=59.5^\circ$), 1.47 ($2\theta=62.9^\circ$), 1.29 ($2\theta=72.9^\circ$) and 1.27 ($2\theta=74.4^\circ$). The corresponding d (lattice spacing) of the 2θ ($^\circ$) peaks are similar to those determined in the literature [16, 17, 21, 22] for tetragonal crystal zirconia which is the stable phase of zirconia.

SEM

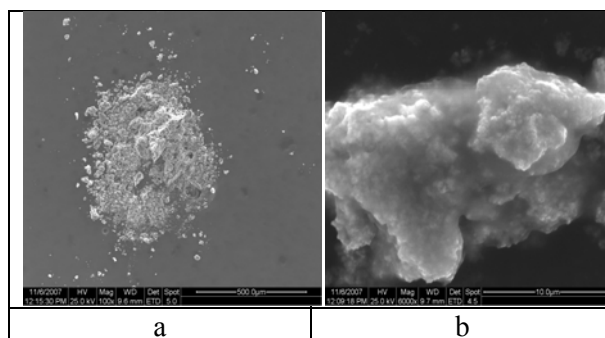


Fig. 3. SEM image of the tetragonal stabilized zirconia (treated with 5M NaOH) after heat treatment at 700 °C: (a) magnification 100x; (b) magnification 6000x.

According to SEM image presented in *Fig. 3 (b)* after heat treatment at 700 °C, the tetragonal stabilized zirconia has large grains with smooth surfaces, approximately spherical in shape.

3.2. PMMA- results

FTIR

Fig. 4 shows the FTIR spectrum of the PMMA.

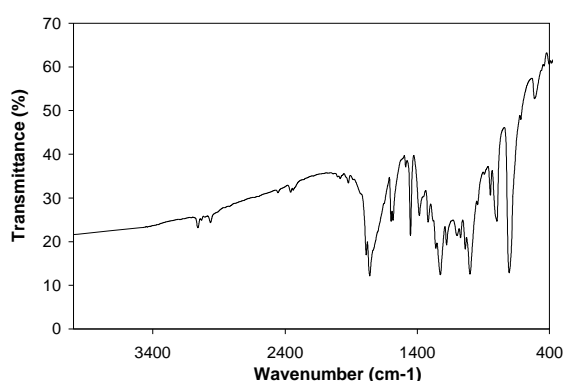


Fig. 4. FTIR spectrum of PMMA.

The characteristic vibration bands of PMMA appear at 1756 cm^{-1} $\nu(\text{C}=\text{O})$ and 1450 cm^{-1} $\nu(\text{C}-\text{O})$. The bands at 3055 and 2959 cm^{-1} correspond to the C-H stretching of the methyl group (CH_3) and the bands at 1382 and 1450 cm^{-1} are associated with C-H symmetric and asymmetric stretching modes, respectively. The 1244 cm^{-1} band is assigned to torsion of the methylene group (CH_2) and the 1177 cm^{-1} band corresponds to vibration of the ester group C-O, while C-C stretching bands are at 997 and 845 cm^{-1} [23, 24, 25].

XRD

The XRD diffractogram of PMMA beads is shown in *Fig. 5*.

PMMA is known to be an amorphous polymer and shows three broad peaks at 2θ values of 11.62° , 30.67° and 31.96° (d spacing approx. 7.61, 2.91 and 2.79\AA correspondingly) with decreasing intensity. According to literature, the shape of the first most intense peak reflects the ordered packing of polymer chains while the second peak denotes the ordering inside the main chains [23].

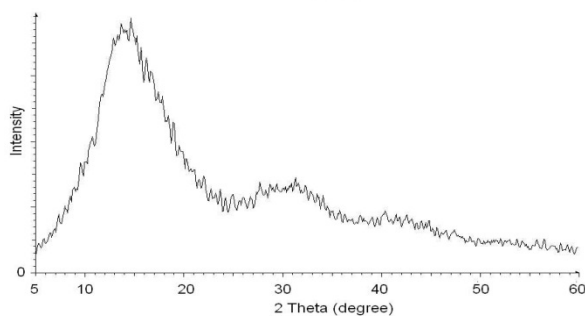


Fig. 5. XRD diffractogram of PMMA beads.

SEM

Fig. 6 shows the SEM image of PMMA beads. As clearly seen, the PMMA beads have a spherical form. The diameter of the most beads is approx. $16\ \mu\text{m}$.

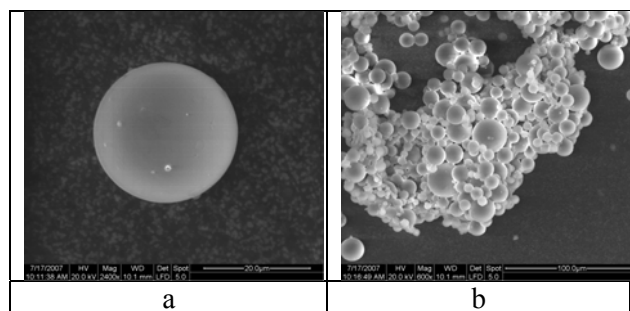


Fig. 6. SEM image of PMMA beads: (a) magnification 2400x; (b) magnification 600x.

3.3 Acrylic bone cement reinforced or not with bioceramic (ZrO_2 powder).- results

FTIR

Fig. 7 shows the FTIR spectra of both acrylic bone cements reinforced with tetragonal zirconia powder or not.

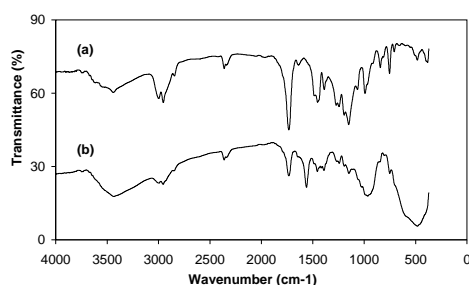


Fig. 7. FTIR spectra of (a) acrylic bone cement without bioceramic (tetragonal zirconia powder in 22.5% w/w) and (b) reinforced with bioceramic (tetragonal zirconia powder in 22.5% w/w).

All the characteristic vibration bands of PMMA. are presented in *Fig. 7 (a)*, and the main characteristic vibration bands of PMMA appear at 1729 cm^{-1} (C=O) and in the fingerprint at 1448 cm^{-1} (C-O) [23, 24, 25].

According to *Fig. 7 (b)*, the presence of tetragonal zirconia powder in the acrylic bone cements is indicated by the peak at 471 cm^{-1} assigned to Zr-O stretching modes [15, 16, 17].

XRD

The XRD diffractogram of the acrylic bone cement without bioceramic (tetragonal zirconia powder in 22.5% w/w) presented in *Fig. 8*, indicate amorphous structure.

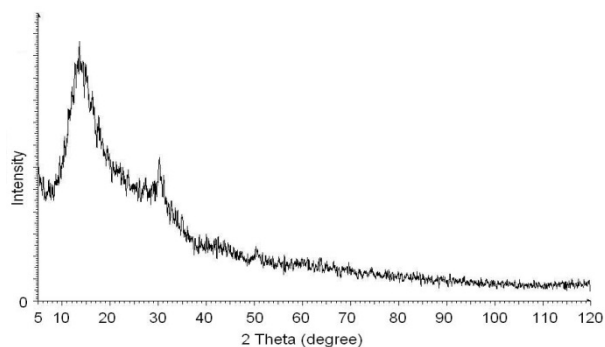


Fig. 8. XRD diffractogram of acrylic bone cement without bioceramic (tetragonal zirconia powder)

Fig. 9 shows the XRD results of the acrylic bone cement reinforced with bioceramic (tetragonal zirconia powder in 22.5% w/w).

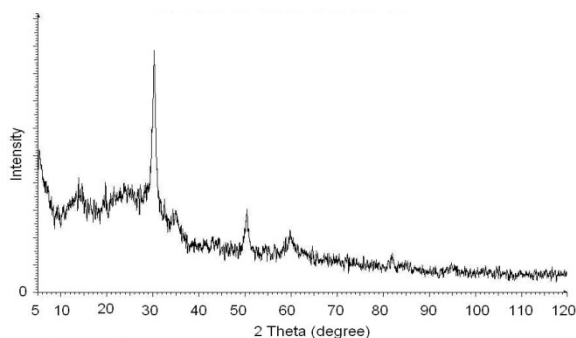


Fig. 9. XRD diffractogram of acrylic bone cement reinforced with bioceramic (tetragonal zirconia powder in 22.5 % w/w).

According to the diffraction peaks of *Fig. 9*, the corresponding d spacings (\AA) were determined: 7.1 ($2\theta=12.3^\circ$), and 2.93 ($2\theta=30.3^\circ$) correspond to PMMA, while the d spacings 2.93 ($2\theta=30.3^\circ$) 2.53 ($2\theta=30.8^\circ$), 2.57 ($2\theta=34.8^\circ$), 2.09 ($2\theta=43.2^\circ$), 1.81 ($2\theta=50.8^\circ$), 1.55

($2\theta=60.3^\circ$), 1.44 ($2\theta=63.1^\circ$) and 1.29 ($2\theta=73.3^\circ$) correspond to tetragonal phase of zirconia powder [16, 17, 21, 22, 23].

SEM

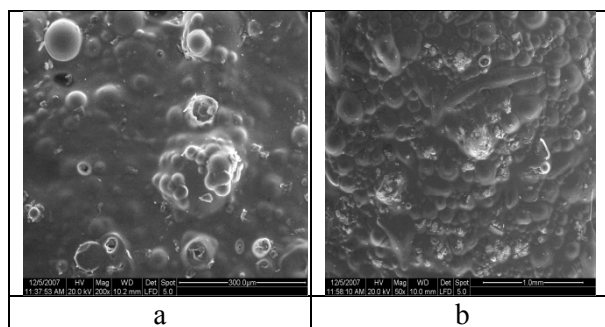


Fig.10. SEM images of (a) acrylic bone cement without bioceramic (tetragonal zirconia powder in 22.5 % w/w) and (b) reinforced with bioceramic (tetragonal zirconia powder in 22.5 % w/w).

According to SEM image presented in *Fig. 10 (a)*, the PMMA beads are distinguished in the acrylic bone cement, with the polymerized MMA connecting the beads.

According to *Fig. 10 (b)*, the acrylic bone cement is a multiphase composite material. The PMMA beads retain their shape and are surrounded by the polymerized MMA monomer acting as binding agent. The small white particles are ZrO_2 powder used as bioceramic.

4. Conclusions

It can be concluded that a suitable acrylic bone cement reinforced with bioceramic (ZrO_2 powder) have been synthesized which can be used as biomaterial candidate. Bioactivation of the PMMA bone cement by adding ZrO_2 powder acting as bioceramic can be an advantageous solution for problems of bone filling as well as bone regeneration.

Acknowledgements

The authors gratefully acknowledge Mr. Loukas Zoumpoulakis, Assistant Professor in the School of Chemical Engineering, Department of Materials Science and Engineering, National Technical University of Athens, for his technical collaboration. Also, the authors would like to thank Prof. A. Vgenopoulos of the School of Mining Engineering and Metallurgy, for kindly helping for FTIR measurements.

References

- [1] S. Daglilar , M.E. Erkan , O. Gunduz , L.S. Ozyegin , S. Salman , S. Agathopoulos , F.N. Oktar, *Materials Letters* **61**, 2295 (2007).
- [2] Alejandro May-Pat, Wilberth Herrera-Kao, Juan V. Cauich-Rodriguez, Jost M. Cervantes-Uc, Sergio G. Flores-Gallardo, *Journal of mechanical behavior of biomedical materials* **2**, 95 (2012).
- [3] E. Rusen, C. Zaharia, T. Zecheru, B. Marculescu, R. Filmon, D. Chappard, R. Badulescu, C. Cincu, *Journal of Biomechanics* **40**, 3349 (2007).
- [4] I. Espigares, C. Elvira, J. F. Mano, B. Vazquez, J. S. Roman, R. L. Reis, *Biomaterials* **23**, 1883 (2002).
- [5] A. M. Moursi, A. V. Winnard, P. L. Winnard, J. J. Lannutti, R. R. Seghi, *Biomaterials* **23**, 133 (2002).
- [6] Fatima Zivic, Miroslav Babic, Nenad Grujovic, Slobodan Mitrovic, Gregory Favaro,

- Mihaela Caunii, Journal of mechanical behavior of biomedical materials **5**, 129-138 (2012).
- [7] Robert J. Kane, Weimin Yue, James J. Mason, Ryan K. Roeder, Journal of mechanical behavior of biomedical materials **3**, 504 (2010)
- [8] S. Deb, L. Aiyathurai, J. A. Roether, Z. B. Luklinska, Biomaterials **26**, 3713 (2005).
- [9] L. Yin, X. F. Song, Y. L. Song, T. Huang, J. Li, International Journal of Machine Tools & Manufacture **46**, 1013 (2006).
- [10] Guocheng Wang, Fanhao Meng, Chuanxian Ding, Paul K Chu, Xuanyong Liu, Acta Biomaterialia **6**, 990–1000 (2010).
- [11] Guocheng Wang, Xuanyong Liu, Chuanxian Ding, Surface & Coatings Technology **202**, 5824–5831(2008).
- [12] G. Aguila, S. Guerrero, F. Gracia, P. Araya, Applied Catalysis A: General **305**, 219 (2006).
- [13] J. Simitzis, D. E. Baciú, J. Optoelectron. Adv. Mater. **14** (5-6),523 (2012).
- [14] J. Simitzis, D. E. Baciú, S. Soulis, M. Tzedaki, J. Optoelectron. Adv. Mater. **12**(5), 1213 (2010)
- [15] X. Bokhimi, A. Morales, O. Novaro, M. Portilla, T. Lopez, F. Tzompantzi, R. Gomez, Journal of solid state chemistry **135**, 28-35 (1998)
- [16] P.N. Kuznetsov, L.I. Kuznetsova, A.M. Zhyzhaev, G.L. Pashkov, V.V. Boldyrev, , Applied Catalysis A: General **227**, 299–307(2002).
- [17] T. Lopez, M. Alvarez, R. Gomez, Journal of Sol-Gel Science and Technology **33**, 93–97, (2005).
- [18] K.G. Kanade, J.O. Baeg, S.K. Apte, T.L. Prakash, B.B. Kale, Materials Research Bulletin **43**, 723–729 (2008).
- [19] Fengxi Chen, Kewu Zhu, Geok Joo Gan, Shoucang Shen, Fethi Kooli, Materials Research Bulletin **42**, 1128–1136 (2007).
- [20] G. Cerrato, S. Bordiga, S. Barbera, C. Morterra, Applied surface science **115**, 53-65 (1997).
- [21] Yang Chunsheng , Wu Qisheng , Liu Yuanyuan, Journal of rare earths **25**, Suppl., 250 (2007).
- [22] H.K. Mishra, K.M. Parida, Applied Catalysis A: General **224**, 179 (2002).
- [23] S. Ahmad, S. Ahmad and S. A. Agnihotry, Bull. Mater. Sci., **30**(1), 31–35 (2007)
© Indian Academy of Sciences.
- [24] C. Parra, Gema Gonzales, C. Albano, e-Polymers, no. **025** (2005).
- [25] S. Rajendran, T. Uma, Bull. Mater. Sci., **23**(1), 27-29, (2000)©Indian Academy of Sciences.